SI Appendix: Charting pathways to climate change mitigation in a coupled socio-climate model.

Thomas Bury[1,2], Chris T. Bauch[1], and Madhur Anand*[2]

[1]Department of Applied Mathematics, University of Waterloo, Waterloo, ON N2L 3G1, Canada
[2]School of Environmental Sciences, University of Guelph, Guelph, ON N1G 2W1, Canada.

*email: manand@uoguelph.ca

1 Socio-Climate Model

We couple an Earth system model (ESM) [11] with reduced ocean dynamics [13], to a dynamic model for social behavior [5, 6, 8]. The full socio-climate model reads

$$\frac{dx}{dt} = \kappa x(1-x)(-\beta + f(T_f) + \delta(2x-1)), \tag{1}$$
$$\frac{dC_{\text{at}}}{dt} = \epsilon(t)(1-x) - P + R_{\text{veg}} + R_{\text{so}} - F_{\text{oc}}, \tag{2}$$
$$\frac{dC_{\text{oc}}}{dt} = F_{\text{oc}}, \tag{3}$$
$$\frac{dC_{\text{veg}}}{dt} = P - R_{\text{veg}} - L, \tag{4}$$
$$\frac{dC_{\text{so}}}{dt} = L - R_{\text{so}}, \tag{5}$$
$$c\frac{dT}{dt} = (F_d - \sigma T^4)a_E. \tag{6}$$

Climate variables are expressed as deviations from pre-industrial levels. Definitions of state variables and climate 'processes' are given in Table 1, and baseline parameter values are provided in Table 2. Functional forms for each process are outlined below.

Photosynthesis

Carbon uptake from the atmosphere via photosynthesis takes the following form

$$P(C_{\text{at}}, T) = k_p C_{\text{ve0}} k_{MM} \left(\frac{\text{pCO}_{2a} - k_c}{K_M + \text{pCO}_{2a} - k_c}\right)\left(\frac{(15+T)^2(25-T)}{5625}\right) \tag{7}$$

for $\text{pCO}_{2a} \geq k_c$ and $-15 \leq T \leq 25$, and zero otherwise. The mixing ratio of CO_2 in the atmosphere, pCO_{2a} is defined as the ratio of moles of CO_2 in the atmosphere to the total number of moles of molecules in the atmosphere k_a. Thus

$$\text{pCO}_{2a} = \frac{f_{\text{gtm}}(C_{\text{at}} + C_{\text{at0}})}{k_a} \tag{8}$$

where $f_{\text{gtm}} = 8.3259 \times 10^{13}$ is the conversion factor from gTC to moles of carbon and C_{at0} is initial level of CO_2 in the atmosphere. Note photosynthesis satisfies Michaelis-Menton kinetics in pCO_{2a} resembling increasing but saturating rates of photosynthesis as carbon in the atmosphere increases. The temperature term captures optimal photosynthesis at $T = 2$ (atmospheric temp. of 27°C) with declining rates for further increases in temperature.

Respiration

Plant respiration takes the form

$$R_{\text{veg}}(T, C_{\text{veg}}) = k_r C_{\text{veg}} k_A e^{-\frac{E_a}{R(T+T_0)}} \tag{9}$$

which increases with the amount of carbon present in the vegetation, and also with the temperature. This provides a positive feedback with increasing carbon levels. Soil respiration takes an analogous form:

$$R_{\text{so}}(T, C_{\text{so}}) = k_{sr} C_{\text{so}} k_B e^{-\frac{308.56}{T+T_0-227.13}}. \tag{10}$$

Turnover

There is an assumed constant fraction of plants dying in a given unit of time:

$$L(C_{\text{veg}}) = k_t C_{\text{veg}} \tag{11}$$

The stored carbon is then fed into the soil reservoir.

Ocean flux

Flux of CO_2 from the atmosphere to the ocean takes the form

$$F_{\text{oc}}(C_{\text{at}}, C_{\text{oc}}) = F_0 \chi \left(C_{\text{at}} - \zeta \frac{C_{\text{at0}}}{C_{\text{oc0}}} C_{\text{oc}} \right) \tag{12}$$

where χ is characteristic solubility of CO_2 in water and ζ is the evasion factor [13]. More complex ocean models couple these parameters to chemical dynamics within the ocean itself [11], however we find good agreement when comparing this simplified climate model with the full Earth system model presented in [11].

Atmospheric Dynamics

We use the "grey-atmosphere approximation" as used in [11] to model atmospheric dynamics. This framework captures changes in global average surface temperature due to changes in albedo, solar flux, and the opacity of CO_2, H_2O_v and CH_4. The net downward flux of radiation absorbed at the planet's surface is given by

$$F_d = \frac{(1-A)S}{4} \left(1 + \frac{3}{4}\tau \right), \tag{13}$$

where A is the surface albedo, S is the incoming solar flux and τ vertical opacity of the greenhouse atmosphere. Expressions for each opacity are given by

$$\tau(\text{CO}_2) = 1.73(\text{pCO}_2)^{0.263} \tag{14}$$

$$\tau(\text{H}_2\text{O}) = 0.0126 \left(H P_0 e^{-(L/RT)} \right)^{0.503} \tag{15}$$

$$\tau(\text{CH}_4) = 0.0231 \tag{16}$$

where pCO_2 is the mixing ratio of CO_2 in the atmosphere as defined earlier, H is the relative humidity, P_0 is the water vapor saturation constant, L is the latent heat per mole of water, and R is the molar gas constant.

2 Parameter Values

2.1 Climate parameters

All climate parameters are borrowed from the Earth System model [11] except for those governing carbon transfer with the ocean, where we use a simplified framework [13]. We calibrate these ocean parameters to recover dynamics of the full Earth System model. The relative humidity H is calibrated to give a pre-industrial temperature of 288.15K. Parameter values along with upper and lower bounds are listed in Table 2.

2.2 Social Parameters

For reference, social dynamics are modeled by

$$\frac{dx}{dt} = \kappa x(1-x)(-\beta + f(T_f) + \delta(2x-1)). \tag{17}$$

Justification for baseline parameters are provided below. The effect of varying key social parameters is detailed in the manuscript.

Social learning rate ($\boldsymbol{\kappa}$) determines the rate at which an alternate strategy propagates throughout a population, once the alternate strategy has a higher overall utility. Population level change in consensus can take decades (e.g. smoking as a health hazard) and so we select a value of κ accordingly. The time taken for consensus change is $O(1/\kappa)$ and so we use a baseline value of $\kappa = 0.05$ to correspond to change over a 20-year period. This is similar to previous studies modeling of evolving population consensus in socio-ecological systems [6, 8]. Upper/lower bounds of κ are taken to correspond population level consensus change from 5 / 50 years respectively.

Net cost of mitigation ($\boldsymbol{\beta}$) is set to one without loss of generality. Other payoff parameters are normalised to be relative to the net cost of mitigation.

Strength of social norms ($\boldsymbol{\delta}$) is a measure of the 'cost' that an individual incurs when acting against the majority opinion. In a population with complete consensus ($x = 1, 0$), the cost to adopt the alternate strategy is exactly δ. We assume this cost is on the same order as the net cost of mitigative practices (β) and so we investigate δ for the range $(0.5, 1.5)$.

Cost of warming ($\boldsymbol{f(T_f)}$) represents the perceived costs associated with a global temperature anomaly of T_f degrees Celsius. Despite the growing acceptance of climate change and its consequences, the rate of global CO_2 emissions per capita shows little sign of slowing down (Figure 8). Temperature records report a current temperature anomaly of 1°C above pre-industrial values and CO_2 emissions per capita are hovering at approximately 1.3 $\mathrm{tC\,yr^{-1}}$, the highest rate in history. When modeling an individual's perceived cost of global warming at a temperature of T, we therefore use a sigmoidal function (Methods). This assumes small temperature anomalies (on the order of 1°C) receive low response, as is observed in empirical data (Figure 8). At a specified threshold temperature, the response function increases in a non-linear fashion, capturing the expected non-linear increase in frequency of climate change disasters as temperature increases [12]. The cost function eventually saturates for high enough temperature.

3 Additional Figures and Tables

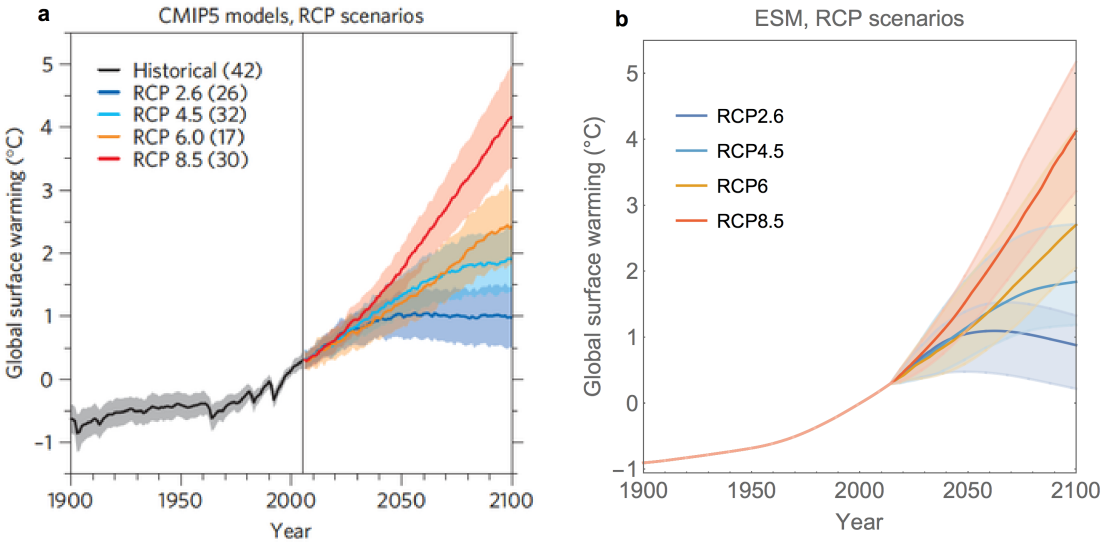

Figure 1: **Comparing temperature projections from the simple Earth system model with those of more complex climate models. a.** Ensemble of simulations from the Coupled Model Intercomparison Project Phase 5 (CMIP5) using the Representative Concentration Pathways (RCPs) as emission scenarios (figure from Knutti et al. [10]). **b.** Ensemble of simulations from the simple Earth system model that we use in our socio-climate model with the same fixed emission trajectories. Parameters are drawn from triangular distributions with upper and lower bounds given in Table 2.

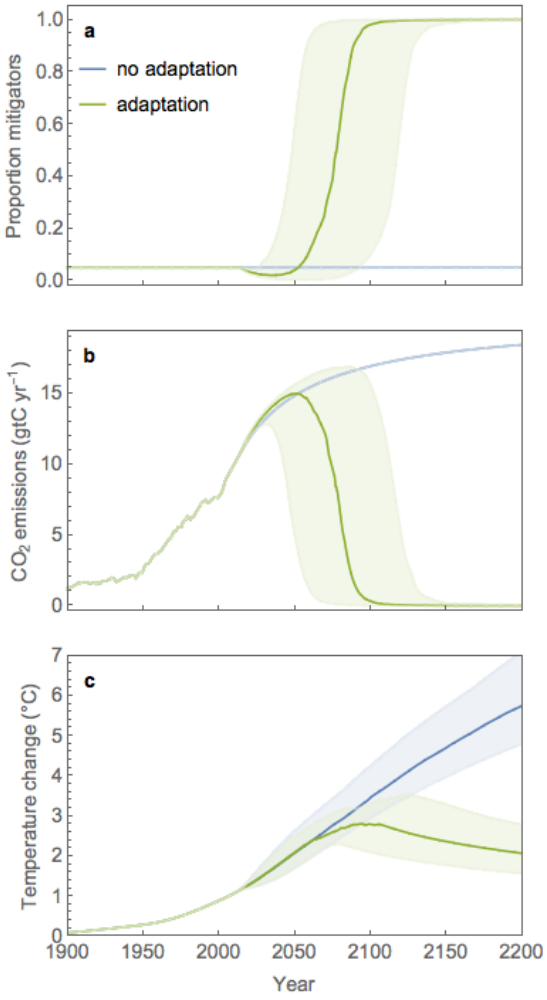

Figure 2: **Climate trends with and without adaptation to climate change.** Removing adaptive behaviour from the model (by forcing the proportion of mitigators to remain at a constant, low value) results in saturating emissions and temperature increasing indefinitely (at least over the next two centuries). This is akin to the RCP8.5 scenario in the latest IPCC report (trajectory shown in Figure 1). Simulations above use parameter values drawn from triangular distributions with upper and lower bounds given in Table 2.

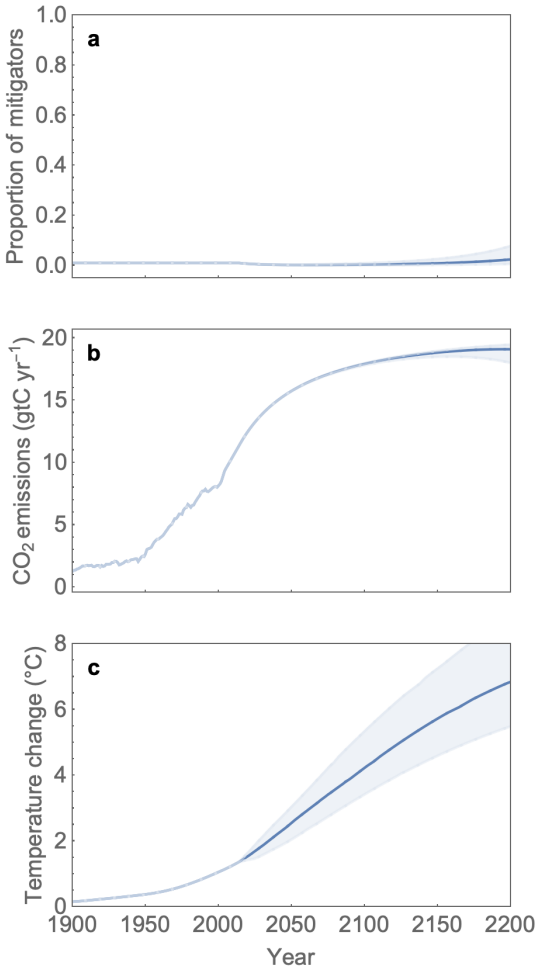

Figure 3: **Worst-case scenario of the coupled socio-climate model.** Setting the social parameters to their bound that most favour non-mitigative behaviour, we get no spread of mitigative behaviour within the considered time-frame. This causes the temperature to increase in a manner similar to the RCP 8.5 scenario (Figure 1). Fixed parameter values are $\kappa = 0.02$, $\beta = 1.5$, $\delta = 1.5$, $f_{\max} = 4$, $x_0 = 0.01$. All other parameter values are drawn from triangular distributions with upper and lower bounds given in Table 2.

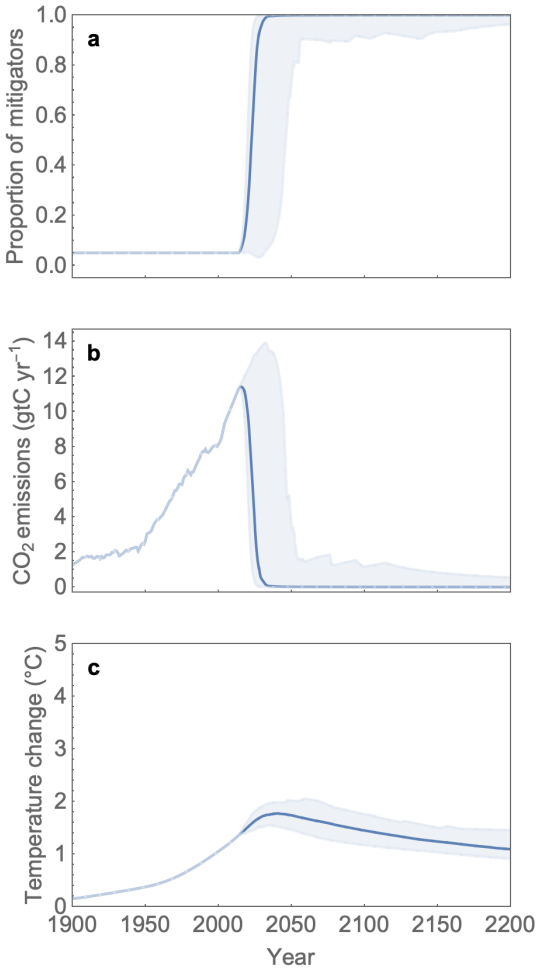

Figure 4: **Best-case scenario of the coupled socio-climate model.** Setting the social parameters to their bound that least favour non-mitigative behaviour, we get very early spread of mitigative behaviour. This causes the temperature to evolve in a manner most similar to the RCP 2.6 scenario where temperature change stays below 2 degrees Celsius (Figure 1). Fixed parameter values are $\kappa = 0.2$, $\beta = 0.5$, $\delta = 0.5$, $f_{\max} = 6$, $t_f = 50$. All other parameter values are drawn from triangular distributions with upper and lower bounds given in Table 2.

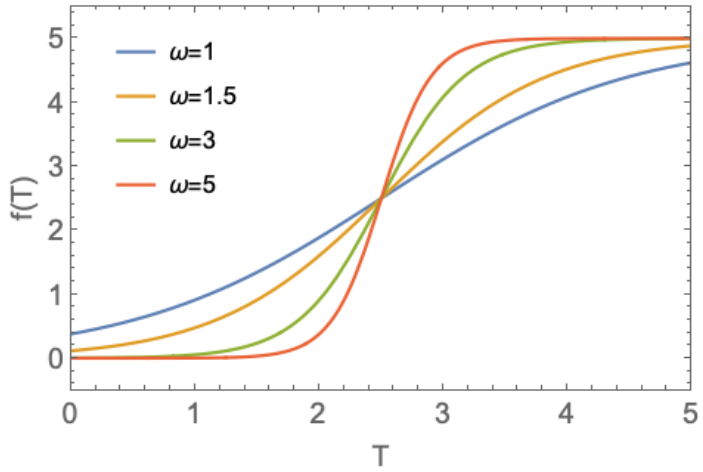

Figure 5: **Functional form for perceived costs associated with climate change.** The incentive of individuals to mitigate is in part based on their perceived costs of climate change f at some projected temperature T. We adopt a sigmoidal response curve for $f(T)$ with variable curvature ω and horizontal shift T_c (the explicit form of $f(T)$ is provided in Methods). This form captures the expected non-linear increase in climate change impacts (cost) as temperature increases.

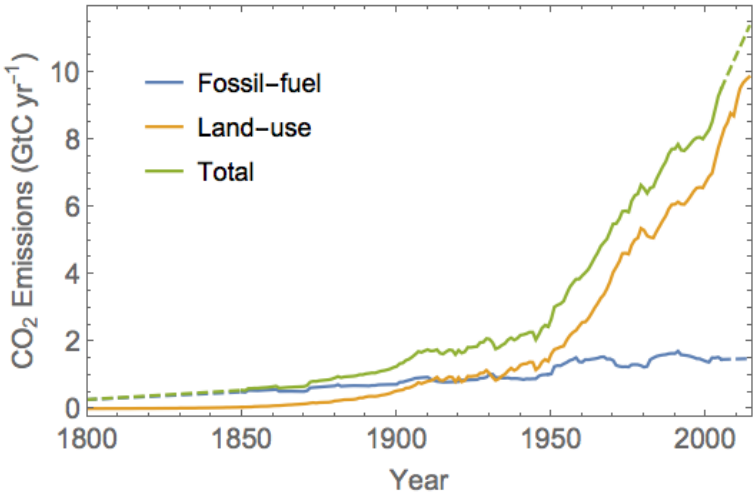

Figure 6: **Estimated historical CO_2 emissions.** Data from the CDIAC on carbon emissions due to fossil-fuel burning and land-use changes, during the years 1800-2014. Land-use data is only available from 1850-2005 and so we linearly extrapolate (dashed line) to match the range of the fossil-fuel data. The sum of the emission trajectories is used to drive the model up to the year 2014, from which point the behavioral component of the socio-climate model is initiated.

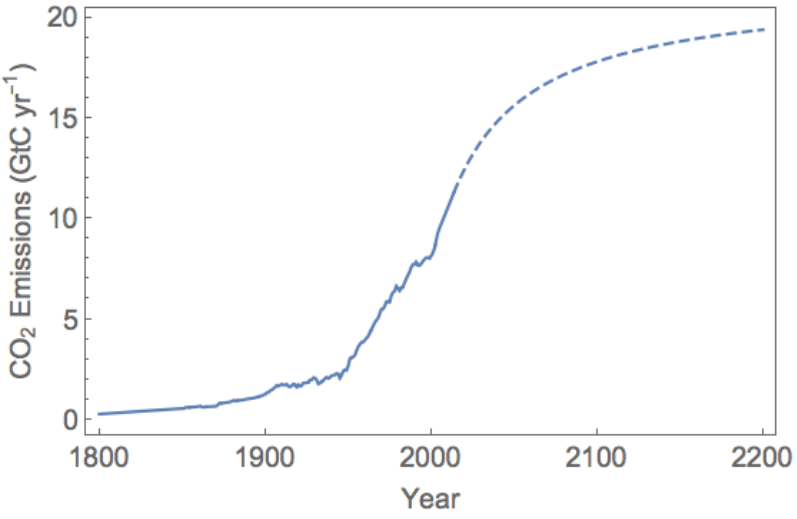

Figure 7: **Emissions in the absence of behavioral change, $\epsilon(t)$.** In the socio-climate model, the factor $\epsilon(t)$ corresponds to the global CO_2 emissions should there be no change in human behavior. Pre 2014, $\epsilon(t)$ takes the historical emission trajectory (solid line) as human behavior is not modeled here. Post 2014, $\epsilon(t)$ follows a saturating function (dashed line) to capture the saturation of global population size and energy needs. Details of this functional form can be found in the Methods section.

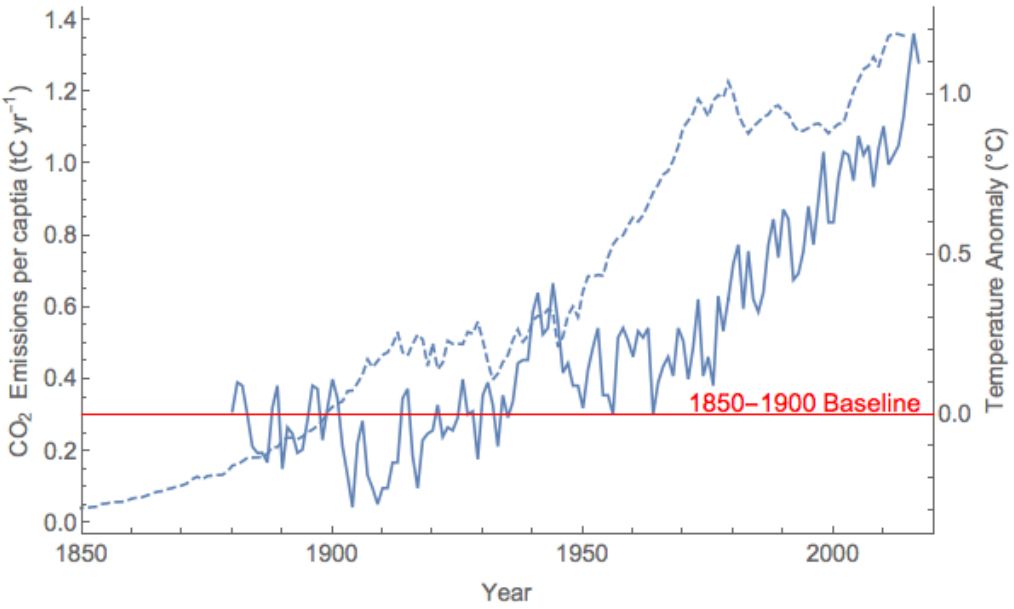

Figure 8: **Comparing per capita CO_2 emissions with global temperature changes.** Temperature anomaly (solid line) above the 1850-1900 baseline value and CO_2 emissions per capita (dashed line) are shown for the 1850-2014. Data was obtained from the CDIAC data repository [1]. It is clear that despite exceeding a 1 degree temperature anomaly, the global emissions per capita of CO_2 show no obvious signs of decreasing. The current temperature anomaly is not yet high enough to spark a global decrease in emissions.

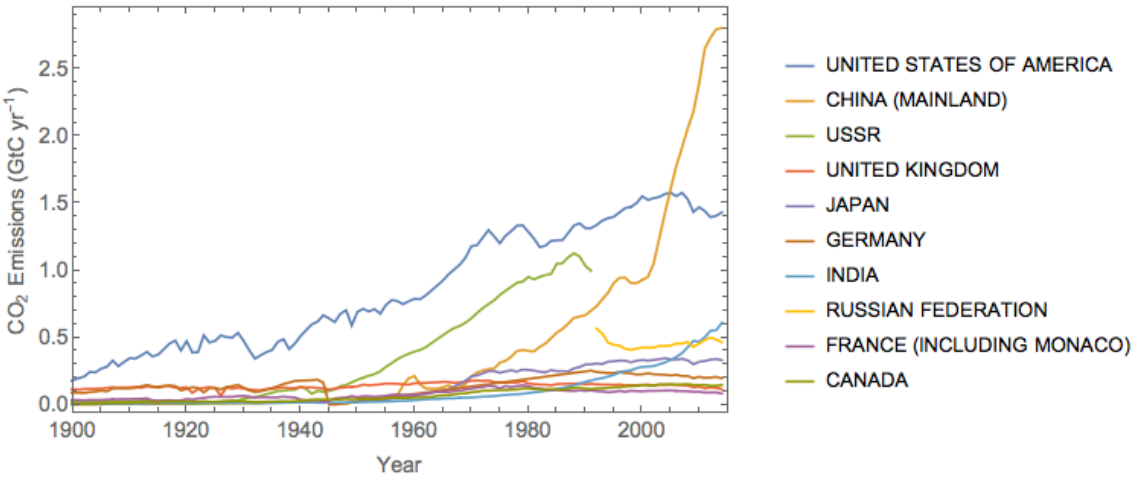

Figure 9: **CO_2 emissions by country.** Total industrial CO2 emissions from the ten countries with the greatest cumulative output. Data was obtained from the CDIAC data repository [1]. Note the termination of the green curve marks the dissolution of the Soviet Union and the beginning of the yellow curve marks the formation of the Russian Federation.

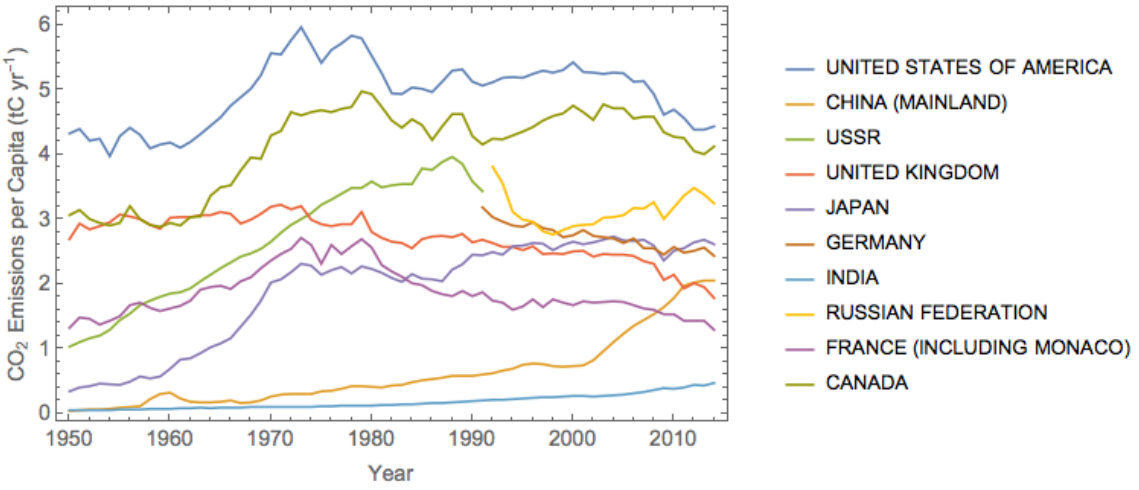

Figure 10: **CO_2 emissions per capita by country.** Total industrial CO_2 emissions per capita from the ten countries with the greatest cumulative output. Data was obtained from the CDIAC data repository [1]. From 1950-1980 we observe strong increases in emissions per capita among most of these countries as is seen globally in Figure 8. Many of the countries peak in 1980 and follow slight downwards trends demonstrating a degree of country-level movement towards mitigation. Globally, this is not the case, however (Figure 8).

Variable / Process	Definition	Unit
x	proportion of mitigators in population	1
C_{at}	deviation of atmospheric CO2 (from pre-industrial 1800)	GtC
C_{oc}	deviation of CO2 in ocean	GtC
C_{veg}	deviation in CO2 in vegetation	GtC
C_{so}	deviation in CO2 in soil	GtC
T	deviation in temperature	K
$\epsilon(t)$	CO_2 emissions in absence of mitigation	GtC/yr
P	carbon uptake from photosynthesis	GtC/yr
R_{veg}	respiration from vegetation	GtC/yr
R_{so}	respiration from soil	GtC/yr
F_{oc}	flux of CO2 from atmosphere to ocean	GtC/yr

Table 1: **Variables and dynamic processes.**

Parameter	Definition	Baseline values / intervals	Unit	Source
C_{at0}	initial CO_2 in atmosphere	$(590, 596, 602)$	GtC	[7, 11]
C_{ao0}	initial CO_2 in ocean reservoir	$(1.4, 1.5, 1.6) \times 10^5$	GtC	[13]
C_{veg0}	initial CO_2 in vegetation reservoir	$(540, 550, 560)$	GtC	[7, 11]
C_{veg0}	initial CO_2 in soil reservoir	$(1480, 1500, 1520)$	GtC	[7, 11]
T_0	initial average atmospheric temperature	$(288, 288.15, 288.3)$	K	[11]
k_p	photosynthesis rate constant	$(0.175, 0.184, 0.193)$	yr^{-1}	[7, 11]
k_{MM}	photosynthesis normalising constant	1.478	1	[11]
k_c	photosynthesis compensation point	$(26, 29, 32) \times 10^{-6}$	1	[4, 11]
K_M	half-saturation point for photosynthesis	$(108, 120, 132) \times 10^{-6}$	1	[11]
k_a	mole volume of atmosphere	1.773×10^{20}	moles	[11, 15]
k_r	plant respiration constant	$(0.0828, 0.092, 0.1012)$	yr^{-1}	[7, 11]
k_A	plant respiration normalising constant	8.7039×10^9	1	[11]
E_a	plant respiration activation energy	$(54.63, 54.83, 55.03)$	J mol^{-1}	[3, 11]
k_{sr}	soil respiration rate constant	$(0.0303, 0.034, 0.037)$	yr^{-1}	[7, 11]
k_B	soil respiration normalising constant	157.072	1	[11]
k_t	turnover rate constant	$(0.0828, 0.092, 0.1012)$	yr^{-1}	[7, 11]
c	specific heat capacity of Earth's surface	$(4.22, 4.69, 5.16) \times 10^{23}$	JK^{-1}	[7, 11]
a_E	Earth's surface area	5.101×10^{14}	m^2	universal
σ	Stefan-Boltzman constant	5.67×10^{-8}	$\text{Wm}^{-2}\text{K}^{-4}$	universal
L	latent heat per mole of water	43 655	mol^{-1}	universal
R	molar gas constant	8.314	$\text{J mol}^{-1}\ \text{K}^{-1}$	universal
H	relative humidity	0.5915	1	calibrated
A	surface albedo	$(0.203, 0.225, 0.248)$	yr^{-1}	[9, 11]
S	solar flux	$(1231, 1368, 1504)$	Wm^{-2}	[9, 11]
$\tau(CH_4)$	methane opacity	$(0.0208, 0.0231, 0.0254)$	1	[2, 11]
P_0	water vapor saturation constant	$(1.26, 1.4, 1.54) \times 10^{11}$	Pa	[11, 14]
F_0	ocean flux rate constant	$(2.25, 2.5, 2.75) \times 10^{-2}$	yr^{-1}	[13]
χ	characteristic CO_2 solubility	$(0.2, 0.3, 0.4)$	1	calibrated
ζ	evasion factor	$(40, 50, 60)$	1	calibrated
κ	social learning rate	$(0.02, 0.05, 0.2)$	yr^{-1}	-
β	net cost of mitigation	$(0.5, 1, 1.5)$	1	-
δ	strength of social norms	$(0.5, 1, 1.5)$	1	-
$f_{\max}$	maximum of warming cost function $f(T)$	(4,5,6)	1	-
ω	nonlinearity of warming cost function $f(T)$	$(1, 3, 5)$	K^{-1}	-
T_c	critical temperature of $f(T)$	$(2.4, 2.5, 2.6)$	K	-
t_p	# previous years used for temperature projection	10	yr	-
t_f	# years ahead for temperature projection	$(0, 25, 50)$	yr	-
s	half-saturation time for $\epsilon(t)$ from 2014	$(30, 50, 70)$	yr	-
$\epsilon_{\max}$	maximum change in $\epsilon(t)$ from 2014	$(4.2, 7, 9.8)$	GtC yr^{-1}	-
x_0	initial proportion of mitigators	$(0.01, 0.05, 0.1)$	1	-

Table 2: **Parameter values and definitions.** Parameters values given as a tuple provide the lower bound, baseline, and upper bound values respectively.

References

[1] TA Boden, RJ Andres, and Gregg Marland. Global, regional, and national fossil-fuel co2 emissions (1751-2014)(v. 2017). Technical report, Carbon Dioxide Information Analysis Center (CDIAC), Oak Ridge National . . . , 2017.

[2] Jérôme Chappellaz, JM Barnola, D Raynaud, Ye S Korotkevich, and C Lorius. Ice-core record of atmospheric methane over the past 160,000 years. *Nature*, 345(6271):127, 1990.

[3] AD Friend, AK Stevens, RG Knox, and MGR Cannell. A process-based, terrestrial biosphere model of ecosystem dynamics (hybrid v3. 0). *Ecological Modelling*, 95(2-3):249–287, 1997.

[4] Roger M Gifford. Implications of co 2 effects on vegetation for the global carbon budget. In *The global carbon cycle*, pages 159–199. Springer, 1993.

[5] Dirk Helbing. *Quantitative sociodynamics: stochastic methods and models of social interaction processes*. Springer Science & Business Media, 2010.

[6] Kirsten A Henderson, Chris T Bauch, and Madhur Anand. Alternative stable states and the sustainability of forests, grasslands, and agriculture. *Proceedings of the National Academy of Sciences*, 113(51):14552–14559, 2016.

[7] John T Houghton. *Climate change 1995: The science of climate change: contribution of working group I to the second assessment report of the Intergovernmental Panel on Climate Change*, volume 2. Cambridge University Press, 1996.

[8] Clinton Innes, Madhur Anand, and Chris T Bauch. The impact of human-environment interactions on the stability of forest-grassland mosaic ecosystems. *Scientific reports*, 3:2689, 2013.

[9] James F Kasting, Daniel P Whitmire, and Ray T Reynolds. Habitable zones around main sequence stars. *Icarus*, 101(1):108–128, 1993.

[10] Reto Knutti and Jan Sedláček. Robustness and uncertainties in the new cmip5 climate model projections. *Nature Climate Change*, 3(4):369, 2013.

[11] Timothy M Lenton. Land and ocean carbon cycle feedback effects on global warming in a simple earth system model. *Tellus B: Chemical and Physical Meteorology*, 52(5):1159–1188, 2000.

[12] Timothy M Lenton, Hermann Held, Elmar Kriegler, Jim W Hall, Wolfgang Lucht, Stefan Rahmstorf, and Hans Joachim Schellnhuber. Tipping elements in the earth's climate system. *Proceedings of the national Academy of Sciences*, 105(6):1786–1793, 2008.

[13] KE Muryshev, AV Eliseev, II Mokhov, and AV Timazhev. A lag between temperature and atmospheric co2 concentration based on a simple coupled model of climate and the carbon cycle. In *Doklady Earth Sciences*, volume 463, pages 863–867. Springer, 2015.

[14] Shinichi Nakajima, Yoshi-Yuki Hayashi, and Yutaka Abe. A study on the "runaway greenhouse effect" with a one-dimensional radiative–convective equilibrium model. *Journal of the Atmospheric Sciences*, 49(23):2256–2266, 1992.

[15] JR Toggweiler and Jorge L Sarmiento. Glacial to interglacial changes in atmospheric carbon dioxide: The critical role of ocean surface water in high latitudes. *The carbon cycle and atmospheric CO2: natural variations archean to present*, 32:163–184, 1985.